Pseudomonas germanica sp. nov., isolated from *Iris germanica* rhizomes

Kostadin Evgeniev Atanasov[1,2], David Miñana-Galbis[3], Julia Gallego[4], Annabel Serpico[4], Montserrat Bosch[4], Teresa Altabella[1,2] and Albert Ferrer[1,5]

[1]Center for Research in Agricultural Genomics (CSIC-IRTA-UAB-UB), Bellaterra, Barcelona, Spain.

[2]Department of Biology, Healthcare and the Environment, Plant Physiology Section, Faculty of Pharmacy and Food Sciences, University of Barcelona, Spain.

[3]Department of Biology, Healthcare and the Environment, Microbiology Section, Faculty of Pharmacy and Food Sciences, University of Barcelona, Spain.

[4]Applied Microbiology and Biotechnology Unit, LEITAT Technological Center, Terrassa, Spain.

[5]Department of Biochemistry and Physiology, Faculty of Pharmacy and Food Sciences, University of Barcelona, Spain.

Corresponding author: Kostadin E. Atanasov

The email address for the corresponding author: kostadin.atanasov@cragenomica.es

Keywords: *Pseudomonas*, *Iris germanica*, endophyte, multilocus sequence analysis, type-strain, average nucleotide identity, digital DNA-DNA hybridization.

Repositories:

BioProject: PRJNA705867; BioSample: SAMN18105273; Sequence Read Archive (SRA): SRR14429882; Assembly: ASM1961465v1; GenBank: MZ758888.1.

ABSTRACT

Through bacterial plant-endophyte extraction from rhizomes of *Iris germanica* plant, a Gram-negative, aerobic, catalase and oxidase positive gammaproteobacterial referred to as FIT28^T, was isolated. Strain FIT28^T shows vigorous growth on nutrient rich media within the temperature ranging from 4 to 35 ºC, with optimal growth at 28 ºC, a wide pH adaptation from pH 5 to 11, and salt tolerance up to 6% (w/v) NaCl. Colonies are white-yellow and quickly become mucoid. Analysis of 16S rRNA gene sequence placed the strain within the *Pseudomonas* genus, and multilocus sequence analysis (MLSA) using 16S rRNA, *rpoB*, *gyrB* and *rpoD* concatenated sequence revealed that the closest relatives of FIT28^T are *Pseudomonas zeae* OE48.2^T, *Pseudomonas crudilactis* UCMA 17988^T, *Pseudomonas tensinigenes* ZA5.3^T, *Pseudomonas helmanticensis* OHA11^T, *Pseudomonas baetica* a390^T, *Pseudomonas iridis* P42^T, *Pseudomonas atagonensis* PS14^T, and *Pseudomonas koreensis* Ps 9-14^T, within the *Pseudomonas koreensis* subgroup of the *Pseudomonas fluorescens* lineage. Strain FIT28^T genome size is about 6.7 Mb with 59.09% GC content. Average nucleotide identity (ANI) and digital DNA-DNA hybridization (dDDH) values calculated from the genomic sequences of FIT28^T, and the closely related *P. zeae* OE48.2 type-species are 95.23% and 63.4%, respectively. Biochemical, metabolic, and chemotaxonomic studies further support our proposal that *Pseudomonas germanica* sp. nov., should be considered a novel species of the genus *Pseudomonas*. Hence, the type strain FIT28^T (= LMG 32353^T = DSM 112698^T) was deposited in public cell-type culture centers.

Introduction

Pseudomonas Migula 1894 is a widely distributed genus of rod-shaped gram-negative gammaproteobacteria with monotrichous or lophotrichous flagella. These bacteria are aerobic and have catalase and cytochrome C oxidase activity. Furthermore, they exhibit good growth in nutrient-rich media, salt tolerance, and growth within a range of pH (between 5 and 10). Niches where *Pseudomonas* can be found are diverse and include environmental soil samples, hot spring water, river and lake samples, wastewater, and in association with living organisms. Up to date, the genus contains 270 published species with accepted correct names (www.bacterio.net). Because *Pseudomonas* is one of the most complex genera, during last decades different genetic and genome-based taxonomic methods have been tested in order to identify and classify taxonomically novel isolated *Pseudomonas* species. Multilocus sequence analysis (MLSA) is a gene-based technique where 16S rRNA gene sequence is combined with other protein-coding housekeeping genes such as *rpoB*, *gyrB* and *rpoD*, resulting in a unique concatenated large sequence which is aligned to other species in order to investigate phylogenetic relationship. In 2018, Peix et al., conducted MLSA study on *Pseudomonas* species and outputted a phylogenetic analysis describing species clustering in lineages and groups. Authors suggested the existence of *P. fluorescens* lineage, *P. aeruginosa* lineage, and *P. pertucinogena* lineage. Among them, the groups integrating the most species-abundant *P. fluorescens* lineage were *P. fluorescens*, *P. lutea*, *P. syringae*, *P. rhizosphaerae*, *P. putida*, *P. anguilliseptica*, and *P. straminea* group [1]. Nowadays, the increasing number of fully sequenced genomes enable *in silico* global genome comparisons analysis. Comparative genomics of different species is demonstrating higher accuracy in species-species delineation and is prompting to review and reclassify some taxon species initially considered different but belonging to the same species or subspecies. Pan-genome tools for *in silico* analysis algorithms are average nucleotide identity (ANI), orthologous ANI (orthoANI), blast-based ANI (ANIb),

MUMer3-based ANI (ANIm), USEARCH-based ANI (ANIu), and digital DNA-DNA hybridization (dDDH). ANI and dDDH analysis fix species boundaries percentages at 95 – 96% and 70%, respectively [2]. Hesse et al. (2018) compared genomes of *Pseudomonas* type strains and subspecies by conducting ANI analysis and constructing phylogenetic relationship based on the alignment of protein sequence of orthologous genes. Authors were able to relocate strains from previous MLSA studies [3, 4] and reported subdivision of the *P. fluorescens* group in ten subgroups composed by *P. fragi*, *P. asplenii*, *P. gessardii*, *P. fluorescens*, *P. protegenes*, *P. chlororaphis*, *P. corrugata*, *P. koreensis*, *P. jessenii*, and *P. mandelii* [5]. Nevertheless, despite of the power of gene and genome based-analysis, borderline species identification and delineation are still difficult and can require a combination of exhaustive biochemical, physicochemical, and molecular characterization [6].

Species of the *P. fluorescens* group are soil-born bacteria that are highly associated with plants organisms. However, increasing data are suggesting that some species could infect animals and/or produce infections [7]. Relationship with the plant host can be neutral, pathogenic, or even beneficial by stimulating plant growth and development through diverse molecular mechanism [8]. Pseudomonades are capable to synthetize a broad spectrum of specialized bioactive metabolites with antimicrobial, antioxidant, anticancer and antifungal activities, among others [9], which makes them interesting as a potential new source of this kind of compounds. Hereafter we describe the characterization of a new *Pseudomonas* species isolated from *Iris germanica* rhizomes. Combination of whole genome sequencing data with biochemical and physicochemical analyses enabled us to propose *Pseudomonas germanica* strain FIT28^{T} as a new type-strain.

Isolation and Ecology

Strain FIT28^{T} was isolated from the endosphere of *Iris germanica* rhizomes at the Marimurtra Botanical Garden of Blanes in Catalonia (Spain). Entire plants were collected and examined

for pathogenic lesions, injuries, or the presence of active infections. Only fully healthy plants were used for endophytes extraction. Soil attached to *I. germanica* rhizomes was first washed off with sterile distilled water and next with phosphate buffered saline (PBS; 1.8 mM KH_2PO_4, 10 mM Na_2HPO_4, 2.7 mM KCl, 137 mM NaCl, pH 7.4). Surface sterilization was performed by washing rhizomes with 70% ethanol for 5 min, 2% (w/v) sodium hypochlorite for 10 min, and 70% ethanol for 45 min. Rhizomes were then washed up to seven times with sterile-distilled water. Sterilized rhizomes were dried with paper towel under sterile conditions, transferred to a mortar, and homogenized with pestle in PBS solution. A serial dilution of the crude extract was prepared and 50 µl plated on Tryptic Soy Agar medium (TSA, Sigma-Aldrich, St Louis, USA). Plates were incubated at 30 ºC for 15 days and individual colonies were transferred on new TSA plates and spreaded by extenuation. A single colony was inoculated into 5 ml Tryptic Soy Broth (TSB, Becton Dickinson, Franklin Lakes, USA) medium and incubated for 24h – 72h at room temperature. Endophyte culture was mixed with glycerol up to 25% (v/v) final concentration and stored at -80 ºC.

Multilocus Sequence Analysis (MLSA) and Genome Features

A single colony grown on TSA was transferred to TSB medium and incubated for 16h at 28 ºC, with constant shaking at 190 rpm. Cells were pelleted and DNA extracted by a modified CTAB protocol [10, 11]. For the phylogenetic genus location of strain FIT28^T, PCR amplification of 16S rRNA V5/V6/V7 regions was carried out with 799F (5'-AACMGGATTAGATACCCKG-3') and 1193R (5'-ACGTCATCCCCACCTTCC-3') primers [12]. Five microliters of the PCR reaction were treated with ExoSAP-IT (Thermo Fisher Scientific, Waltham, USA) and sequenced for triplicate. A consensus sequence was generated and a preliminary taxonomic location of strain FIT28^T stablished by nucleotide-blast analysis against the bacterial 16S rRNA database of NCBI and the Ribosomal Database Project (RDP; http://rdp.cme.msu.edu/) [13].

For high-quality genomic DNA isolation, 20 ml of a strain FIT28^T culture in TSB was used. DNA extraction was performed with Wizard Genomic DNA Extraction Kit (Promega, Madison, USA). Two hundred microliters of genomic crude extract were treated for 30 min with 3 µl of 10 mg·ml^{-1} RNase A DNase free (Panreac AppliChem, Darmstadt, Germany), and then deproteinized by chloroform-isoamyl alcohol treatment, followed by a 70% ethanol wash and resuspended in 300 µl of nuclease free water. DNA was passed through Genomic DNA Clean & Concentrator-10 column (Zymo Research, Irvin, USA) and eluted in TE buffer according to manufacturer instructions. DNA was quantified by Qubit 3.0 fluorometer (Life Technologies, Carlsbad, USA), and the DNA integrity number (DIN) was assessed with Bioanalyzer DNA 12000 chip (Agilent, Santa Clara, USA). Whole genome sequencing of strain FIT28^T was performed with Illumina Novaseq (2x150 bp) and PacBio RSII platforms. Achieved genome coverage was 495 times. Illumina and PacBio sequencing reads were used to construct a hybrid genome assembly using Unicycler v0.4.8 [14].

Genome annotation was performed with the Prodigal pipeline in order to identify protein coding genes [15]. Genome contamination was screened with ContEst16S [16]. Ribosomal 16S rRNA genes were predicted on assembled contigs using Barnnap (https://github.com/tseemann/barrnap). A consensus sequence of the ribosomal 16S RNA gene of strain FIT28^T was extracted and analyzed with the taxonomically united database of EzBioCloud [17]. Search was limited to bacterial type strains and genome assemblies of related species downloaded from GenBank database. For MLSA we used sequences of the housekeeping *rpoB*, *gyrB* and *rpoD* genes (Table S1) [18]. Sequences of 16S rRNA, *rpoB*, *gyrB*, and *rpoD* were extracted from genome assemblies, concatenated, and aligned with MUSCLE algorithm [19]. Genome assemblies for *P. defluvii* WHCP16^T and *P. turukhanskensis* IB1.1^T were not available at the moment of writing this paper. For *P. helmanticensis* OHA11^T (= CECT 8548^T = LMG 28168^T) raw genome assembly was

downloaded from the JGI Genome Portal [20]. Genomes of *P. helmanticensis* OHA11^T, *P. zeae* OE 48.2^T, *P. tensinigenes* ZA 5.3^T, *P. iridis* P42^T, and *P. hamedanensis* SWRI65^T, were annotated with PATRIC 3.6.9 [21] and sequences for MLSA extracted from gene annotation. A total number of 41 species were considered for the study. We used *P. aeruginosa* DSM 50071^T as a rooting outgroup. Neighbor-Joining trees were generated with Mega 10 software [22]. Afterwards, distance matrices were calculated by the Jukes-Cantor method and bootstrap analysis was performed based on 1000 re-sampling [23]. Gaps or missing data were treated by pairwise deletion.

Comparison of 16S rRNA phylogenetic analysis located strain FIT28^T with *P. zeae* OE48.2^T (99.87%), *P. tensinigenes* ZA5.3^T (99.87%), *P. helmanticensis* OHA11^T (99.86%), *P. hamedanensis* SWRI65^T (99.67%), *P. crudilactis* UCMA 17988^T (99.61%), *P. atagonensis* PS14^T (99.59%), *P. baetica* a390^T (99.52%), and *P. iridis* P42^T (Fig. S1.1). Nucleotide-blast and pairwise alignment (https://blast.ncbi.nlm.nih.gov/) of the concatenated housekeeping genes outputted next sequence identities: 98.98% (*P. zeae* OE48.2^T), 98.91% (*P. tensinigenes* ZA5.3^T), 96.96% (*P. helmanticensis* OHA11^T), 97.52% (*P. hamedanensis* SWRI65^T), 98.50% (*P. crudilactis* UCMA 17988^T), 97.24% (*P. atagonensis* PS14^T), 96.10% (*P. baetica* a390^T), and 96.27% (*P. iridis* P42^T)(Table S2). Similar results were obtained when we included additional housekeeping genes *corA*, *atpD* and *recA* [24]. Concatenated sequence of 16S rRNA, *rpoB*, *gyrB*, *rpoD*, *corA*, *atpD* and *recA* genes were aligned with 98.98% of sequence identity, 92% of coverage, between FIT28^T and *P. zeae* OE48.2^T. 98.44% identity was observed when 16S rRNA, *corA*, *atpD* and *recA* where used, but in this case, sequence coverage dropped down to 79%. Furthermore, up-to-date bacterial core gene (UBCG) [25] analysis was carried out by aligning 91 concatenated core genes where 50 out of UBCGs supported FIT28^T and *P. zeae* OE48.2^T phylogenetic relationship with 98.01% of sequence

identity (Fig. S1.2). These values were slightly above the threshold of 97% purposed in MLSA for the species boundary [3, 24, 26].

Nevertheless, MLSA based phylogenetic-tree helped to define a thirteen-member clade formed by strains FIT28^T, *P. zeae* OE48.2^T, *P. crudilactis* UCMA 17988^T, *P. tensinigenes* ZA5.3^T, *P. helmanticensis* LMG 28168^T (= OHA11^T), *P. baetica* LMG 25716^T (= a390^T), *P. iridis* P42^T, *P. atagonensis* PS14^T, *P. koreensis* DSM 16610^T, *P. granadensis* LMG 27940^T, *P. hamedanensis* SWRI65^T, *P. atacamensis* M7D^T, and *P. moravienis* BS3668^T (Figure 1) which was considered in order to define inter-strain comparisons. Hence, in concordance to the previous phylogenetic data we propose that strain FIT28^T can represent a new member of the *P. koreensis* subgroup within the *P. fluorescence* group of the homonym lineage.

In silico prediction of GC content reported a value of 59.09%, which is characteristic for *Pseudomonas fluorescens* environmental strains [27]. Genome size was 6.713.530 base-pair (bp), with predicted 6.022 protein coding genes [28], 19 rRNA coding genes, including 5S rRNAs (7 genes), 16S rRNAs (6 genes), and 23S rRNAs (6 genes), and 75 tRNA coding genes [29]. Based on MLSA analysis we selected thirteen-member clade species (Figure 1) for whole genome comparison. Average nucleotide identity and orthoANI values were calculated by pairwise comparison with Ortho ANI Tool [30]. Blast-based ANI (ANIb) and MUMmer3 ANI (ANIm) were tested by JSpeciesWS [31], whereas USEARCH ANI (ANIu) was calculated according to Yoon and colleagues [31]. Strain FIT28^T exhibited ANI and orthoANI values of 95.23% and 95.51% (over 64% of genome coverage), respectively, to *P. zeae* OE48.2^T (Table 1, Table S3). ANIu and ANIm values were close to the original ANI and OrthoANI with percentages of 95.92% and 95.44%, respectively. Again, ANIb revealed an average value of 94.94% with genome coverage of 85.84%. Overall, ANI results remained inconclusive due to values within the borderline interval for the generally recommended threshold of 95 – 96% for considering same species [2, 32]. Hence, like in MLSA, genomic analysis was not enough to

194 fully differentiate between these two closely related species. Finally, dDDH analysis was
195 assessed with the Genome-to-Genome Distance Calculator (GGDC) from the DSMZ webtool
196 (https://ggdc-test.dsmz.de/ggdc.php#) with the BLAST+ local alignment algorithm [33]. We
197 used formula 2, which consists of the number of identities within high-scoring segment pairs
198 (HSPs) per total HSP length [34]. The recorded dDDH value for the nearest *P. zeae* OE48.2^T
199 was 63.4% with an 95% of confidence interval of 60.5% - 66.2%, whereas other species
200 exhibited absolute dDDH values between 33.3% (*P. moraviensis* BS3668^T) and 46.7% (*P.*
201 *tensinigenes* ZA5.3^T) (Table 2). Thus, values are clearly below 70% sequence identity, which
202 is considered as the gold standard for new species delineation [2].
203 **Physiology and Chemotaxonomy**
204 A colony of strain FIT28^T grown on TSA medium was placed and immobilized on a
205 microscope glass slide by heat treatment. A Gram stain procedure was performed with a Gram
206 stain set according to manufacturer instructions (Condalab, Torrejón de Ardoz, Spain). Gram
207 negative stained cells were examined with Zeiss Axiophot FL microscope under bright field,
208 and image acquired with Olympus DP70 at the core facilities of the Center for Research in
209 Agricultural Genomics - CRAG (Figure S2). Moreover, a negative stain with uranyl acetate
210 was performed on strain FIT28^T and cells visualized with transmission electron microscope
211 (TEM) Bioscan Gatan, JEOL 1010, at the Scientific and Technological Centers (CCiT) of the
212 University of Barcelona. Strain FIT28^T possess a single polar flagellum and confirmed rod-
213 shaped cells. The estimated cell size was 2.3 μm length per 0.91 μm width (Figure 2).
214 In order to stablish optimal temperature growth conditions, strain FIT28^T was cultured on TSA
215 medium at temperatures ranging from 4 to 40 ºC. Cell growth was observed from 4 to 35 ºC
216 with an optimal temperature stablished at 28 ºC, which agrees with previous reports for
217 environmental *P. fluorescens* species [35]. For pH tolerance, growth was recorded within the
218 range of pH 5-11 at 28 ºC with an optimal pH range from 6 to 7. Production of fluorescent

pigment was tested by culturing on King's B medium (Duchefa Biochemie, Haarlem, the Netherlands) for 24h and image acquisition under 365 nm UV light irradiation [36]. Catalase activity was detected by placing drops of 3% (v/v) hydrogen peroxide solution on active bacterial cell cultures. Bubbles formation was observed when applied to strain FIT28^T, *P. helmanticensis* CECT 8548^T (= OHA11^T), *P. baetica* CECT 7720^T (= a390^T), and *P. atagonensis* CECT 9940^T (= PS14^T), thus indicating positive catalase activity as is in agreement with previously described data. Oxidase activity was also tested on same species as for catalase activity. Small amounts of solid-media active cell cultures were placed on paper disc and drops of tetra-methyl-*p*-phenylenediamine dihydrochloride solution were added. Blue-purple color was observed in all cases indicating cytochrome C oxidase activity.

Biochemical characteristics of strain FIT28^T were examined with API 20E and API 20NE (Biomerieux, Marcy-l'Étoile, France). Growth-dependent tests for the utilization of amino acids, organic acids and carbohydrates were performed with API 50CH (Biomerieux). Additionally, phenotypic fingerprinting for carbon source utilization and chemical sensitivity was performed with Biolog GenIII Microplate (Biolog, Inc., Hayward, USA). All enzymatic, physiological, and biochemical analyses were carried out at 30 ºC according to manufacturer instructions. Test results reading and interpretation was achieved by manual method. Principal biochemical activities and physiological features are summarized in Table 3. To build this table, data for *P. helmanticensis* CECT 8548^T, *P. baetica* CECT 7720^T and *P. atagonensis* CECT 9940^T were obtained in this study whereas data for the other species were extracted from literature [37–47]. Salt tolerance was also assessed up to 9% of NaCl (w/v) with a maximum growth-tolerance at 6% NaCl for the isolated strain. This result was corroborated with the miniaturized Biolog's GenIII test recording growth capacity at 6% (w/v) of NaCl for strain FIT28^T. According to this, we found higher salt tolerance for strain FIT28^T when compared to *P. zeae* OE48.2^T, *P. tensinigenes* ZA5.3^T, *P. crudilactis* UCMA 179881^T, *P. helmanticensis*

CECT 8548^T *P. baetica* CECT 7720^T, *P. atagonensis* CECT 9940^T, *P. granadensis* LMG 27940^T, *P. hamedanensis* SWRI65^T, and *P. atacamensis* LMG 34516^T, but similar salt tolerance to *P. iridis* P42^T, *P. koreensis* DSM 16610^T, and *P. moraviensis* DSM 16007^T (Table 3). FIT28^T can utilize as carbon source compounds such as D-arabitol, D-fructose, D-saccharic acid, formic acid, inosine, L-alanine, L-pyroglutamic acid, pectin, propionic acid, sucrose, tween 40, dextrin, D-mannitol, glycyl-L-proline, methylpyruvate, α-hydroxybutiric acid, D-trehalose, D-gluconic acid, L-lactic acid, glycerol, N-acetyl-D-glucosamine, L-histidine, D-malic acid, L-serine, and bromo-succinic acid, while *P. zeae* OE48.2^T exhibits negative or uncertain results for the utilization of those compounds. We also found differences regarding the utilization of D-cellobiose, D-sorbitol, gelatin, D-salicin, α-ketobutyric acid, D-glucose-6-phosphate, D-fructose-6-phosphate, acetoacetic acid, N-acetyl-β-D-mannosamine, 3-methyl glucose, D-turanose, gentiobiose, and stachyose. These compounds were found negative (D-sorbitol and gelatin) or uncertain/weak when FIT28^T was compared to *P. zeae* OE48.2^T data reported by Girard and colleagues [46]. Strain FIT28^T, *P. tensinigenes* ZA5.3^T, *P. crudilactis* UCMA 17988^T, *P. helmanticensis* CECT 8548^T and *P. baetica* CECT 7720^T have melibiose oxidative activity whereas *P. iridis* P42^T, *P. atagonensis* CECT, *P. koreensis* DSM 16610^T and *P. moraviensis* DSM 16007^T were negative for this catabolic process. Oxidation of melibiose was uncertain for *P. zeae* OE48.2^T and *P. hamedanensis* SWRI65^T. We also observed that strain FIT28^T is negative for arabinose oxidation and phenylacetic acid assimilations. Enzymatic activities were screened and FIT28^T exhibited gelatin hydrolysis capacity whereas *P. zeae* OE48.2^T, *P. tensinigenes* ZA5.3^T, *P. crudilactis* UCMA 179881^T, *P. helmanticensis* CECT 8548^T, *P. hamedanensis* SWRI65^T and *P. atacamensis* LMG 34516^T could not. We also observed C14 aliphatic lipase activity in almost all strains and uncertain results for *P. helmanticensis* CECT 8548^T. Strain FIT28^T exhibited aminopeptidase (arylamidase) activity for leucine and valine which has been described to be related with nitrification processes [48].

Trypsin, acid, and alkaline phosphatase activities were also observed. Aliphatic compounds activity was detected by C_{14} lipase, C_4 esterase and C_8 esterase-lipase positive reaction on API Zym (Biomerieux) colorimetric test. Other positive enzymatic activities such as arginine dihydrolase, urease, and naphthol-AS-BI-phosphohydrolase activities were detected too. When we addressed chemical growth tolerance, we also found differences between FIT28^T, *P. zeae* OE48.2^T, and *P. tensinigenes* ZA5.3^T. Strain FIT28^T tolerates fusidic acid and minocycline, whereas *P. zeae* OE48.2^T is uncertain and negative, respectively. FIT28^T is unable to grow in the presence of lithium chloride, guanidine HCl, and D-serine, whereas *P. zeae* OE48.2^T and *P. tensinigenes* ZA5.3^T exhibited tolerance and uncertain result, respectively.

In order to determine cell fatty acids and major polar lipids composition, FIT28^T cell cultures were grown at 28 ºC in 200 ml of TSB medium for 24h, under constant shaking at 190 rpm. Cells were recovered by centrifugation at 4000 rpm for 15 min at 4 ºC. The resulting supernatant was discarded, and cell pellet was resuspended in 0.22 µm sterile-filtered cryo-protectant solution (ATCC Reagent-18) containing 0.75% (w/v) trypticase soy broth, 10% (w/v) sucrose, and 5% (w/v) bovine serum albumin fraction V. Two hundred or 30 mg of freeze-dried cells were used for polar lipids and cellular fatty acids composition analysis, respectively. Results from FIT28^T were compared to biochemical features and data from phylogenetic-related species which were extracted from literature [39, 40, 44, 45, 47, 49, 50]. The most abundant fatty acid in strain FIT28^T is an aliphatic unsaturated chain of 16 carbons ($C_{16:0}$) which represents the 29.6% of the total cellular fatty acids (Table 4). This percentage was slightly lower than that reported for *P. crudilactis* UCMA 179881^T (33.7%), *P. helmanticensis* OHA11^T (31.9%), *P. atagonensis* (32.8%), *P. granadensis* LMG 27940^T (31.9%) and *P. iridis* P42^T (35.97%), very similar to that in *P. baetica* a390^T (29.43%) and *P. moraviensis* DSM 16007^T (28.8%), and clearly higher than in *P. atacamensis* LMG 34516^T (24.98%) and *P. koreensis* DSM 16610^T (20%) which exhibited the lower $C_{16:0}$ content among

the compared strains (Table 4). Major polar lipids were analyzed by two-dimensional thin-layer chromatography (TLC). The major polar lipid species in FIT28^T is phosphatidylethanolamine (Figure 3). Compounds that follow in abundance are diphosphatidylglycerol and phosphatidylglycerol. Finally, only traces of aminolipids, phospholipids and glycolipids were detected (Figure 3). Analysis of lipids and cellular fatty acids were carried out by the Identification Service, Leibniz-Institut DSMZ - Deutsche Sammlung von Mikroorganismen und Zellkulturen GmbH, Braunschweig, Germany.

Description of *Pseudomonas germanica* strain FIT28^T

Pseudomonas germanica (ger.ma'ni.ca L. fem. adj. *germanica,* German, from rhizomes of the *Iris germanica*, the source of isolation of FIT28^T) was isolated from *I. germanica* plant-rhizomes at the Marimurtra Botanical Garden, City of Blanes, Catalonia, Spain. Cells are Gram negative, catalase and cytochrome oxidase positive, and have a monotrichous flagellum, hence its motile capacity. Genome size was estimated at 6.713.530 of base-pairs with GC content of 59.09%. Genome annotation and gene prediction has unveiled 6.022 protein coding genes, 19 genes coding for rRNAs, and 75 genes encoding tRNAs. ANI comparison between *P. germanica* genome and those of the nearest related species revealed 95.23% of identity with *P. zeae* OE48.2^T, 91.50% with *P. tensinigenes* ZA5.3^T, 91.13% with *P. crudilactis* UCMA 179881^T, 88.96% with *P. helmanticensis* OHA11^T, 88.12% with *P. baetica* a390^T, 87.73% with *P. atagonensis* PS14^T, 87.62% with *P. koreensis* DSM 16610^T, 87.38% with *P. iridis* P42^T, 87.21% with *P. granadensis* LMG27940^T, 86.83% with *P. atacamensis* M7D^T and *P. moraviensis* BS3668^T, and 86.64% with *P. hamedanensis* SWRI65^T genomes. Digital DNA-DNA hybridization values were 63.4% to *P. zeae* OE48.2^T, 46.7% to *P. tensinigenes* ZA5.3^T, 45.4% to *P. crudilactis* UCMA 179881^T, 38.6% to *P. helmanticensis* OHA11^T, 36.4% to *P. baetica* a390^T, 35.1% to *P. koreensis* DSM16610^T (phylogenetic subgroup of reference of the *P. fluorescens* group of the homonym species lineage), 35% to *P. atagonensis* PS14^T, 34.7%

to *P. iridis* P42^T, 34.2% to *P. granadensis* LMG 27940^T, 33.8% to *P. atacamensis* M7D^T, 33.5% to *P. hamedanensis* SWRI65^T, and 33.3% to *P. moraviensis* BS3668^T.

Strain FIT28^T exhibits vigorous growth on TSA medium between 4 and 35 ºC with an optimal growth temperature of 28 ºC. Colonies are white-yellow and become mucoid in 16h, and the pH range of tolerance is from 5 to 11, with optimal values between 6 and 7. It tolerates a concentration of sodium chloride up to 6 % (w/v). Carbon source utilization is wide and includes dextrin, D-trehalose, sucrose, N-acetyl-D-glucosamine, α-D-glucose, D-ribose, D-mannose, D-melibiose, D-fructose, D-fucose, inosine, D-mannitol, D-arabitol, glycerol, glycyl-L-proline, L-alanine, L-arginine, L-aspartic acid, L-glutamic acid, L-histidine, L-pyroglutamic acid, L-serine, pectin, D-gluconic acid, glucuronamide, xylose, mucic acid, quinic acid, D-saccharic acid, methyl pyruvate, L-lactic acid, citric acid, α-ketoglutaric acid, D-malic acid, L-malic acid, bromo-succinic acid, tween 40, γ-aminobutyric acid, α-hydroxybutyric acid, β-hydroxy-D,L-butyric acid, propionic acid, acetic acid, and formic acid. Negative oxidation and assimilation were achieved for D-maltose, D-raffinose, β-methyl-D-glucoside, N-acetyl-D-galactosamine, gelatin, N-acetyl neuraminic acid, D-sorbitol, myo-inositol, D-aspartic acid, gelatin, and p-hydroxyphenyl acetic acid. Strain FIT28^T exhibited uncertain results for D-cellobiose, gentiobiose, D-turanose, stachyose, D-salicin, N-acetyl-β-D-mannosamine, 3-methyl glucose, L-fucose, L-rhamnose, D-glucose-6-phosphate, D-fructose-6-phosphate, D-serine, D-galacturonic acid, L-galactonic acid lactone, D-glucuronic acid, D-lactic acid methyl ester, α-ketobutyric acid, and acetoacetic acid. FIT28^T displayed the following enzymatic activities: acid and alkaline phosphatase, C_4 esterase and C_8 esterase, C_{14} lipase, arginine dihydrolase, gelatin hydrolysis, naphthol-AS-BI-phosphohydrolase, trypsin and urease activity, leucine, and valine arylamidase. Regarding the chemical growth tolerance, FIT28^T can grow in presence of aztreonam, troleandomycin, rifamycin SV, minocycline, lincomycin, vancomycin, tetrazolium violet, tetrazolium blue, nalidixic acid, potassium

tellurite, niaproof 4, fusidic acid, and 1% sodium lactate, whereas no growth was recorded for guanidine HCl and lithium chloride. Major cellular fatty acids were $C_{16:0}$, $C_{18:1}$ ω7c, and summed future 3 ($C_{16:1}$ ω7c/$C_{15:0}$ iso 2-OH). Detected polar lipids according to their decreasing abundance were diphosphatidylglycerol, phosphatidylglycerol, aminolipids, phospholipids and glycolipids.

Considering the genomic, physical, and biochemical differences between *P. germanica* and its closest relatives, we expose there is enough data to consider this isolate as a newly discovered bacterial species. The type strain is FIT28^T (LMG 32353^T = DSM 112698^T).

Protologue

16s rRNA sequence, genome assembly and SRA data of *P. germanica* strain FIT28^T was deposited in Genbank of the NCBI public database under the accession number MZ758888.1, ASM1961465v1 and SRR14429882, respectively. All genomic submissions are englobed into BioProject number PRJNA705867, BioSample SAMN18105273. Patric 3.6.9 genome feature annotation of *P. zeae* OE48.2^T, *P. tensinigenes* ZA5.3^T, *P. iridis* P42^T, *P. hamedanensis* SWRI65^T, and *P. helmanticensis* LMG 28168^T, as well, FIT28^T raw genome sequence, 16S rRNA and MLSA gene sequences used for phylogeny were deposited at the Microbiology Society Figshare repository (https://microbiology.figshare.com/).

AUTHOR STATEMENTS

Authors and contributors

Kostadin Evgeniev Atanasov (KA), David Miñana-Galbis (DMG), Teresa Altabella (TA) and Albert Ferrer (AF) designed experiments. KA performed experiments and analyzed data with contribution of DMG, TA, and AF. Julia Gallego (JG) harvested plant material used for endophyte isolation and performed strain isolation. Annabel Serpico (AS) and Montserrat Bosch (MB) designed and supervised JG work. This article was written by KA with contributions of all authors.

Conflicts of interest

Authors declare that there are no conflicts of interest.

Funding information

This work was funded by grants RTC-2017-6431 from FEDER/Ministerio de Ciencia, Innovación y Universidades-Agencia Estatal de Investigación (Spain), 2017SGR710 from the Generalitat de Catalunya, and by the CERCA Programme of the Generalitat de Catalunya. We also acknowledge financial support from the Spanish Ministerio de Economía y Competitividad-Agencia Estatal de Investigación through the "Severo Ochoa Programme for Centres of Excellence in R&D" SEV-2015- 0533 and CEX2019-000902-S.

Acknowledgements

We thank Maria Jesús Montes López from the Department of Biology, Healthcare and Environmental Science of the Faculty of Pharmacy and Food Sciences of the University of Barcelona, for her priceless help during strain biochemical characterization. We also thanks to Leigh A. Riley for help in genome annotation and submission at the NCBI GenBank, Bethesda, Maryland USA

LIST OF FIGURES AND TABLES

Principal figures

Figure 1: Multilocus sequence analysis (MLSA) with entire 16S rRNA, *rpoB*, *gyrB*, and *rpoD* gene sequences. Neighbor-joining tree with pairwise deletion and bootstrap percentages on branches from 1000 replicates.

Figure 2: Uranyl acetate negative stain of *Pseudomonas* sp. strain FIT28^T. Image acquired at 25.000 magnifications.

Figure 3: Thin layer chromatography (TLC) analysis of *Pseudomonas* sp. strain FIT28^T major polar lipids.

Principal tables

Table 1: Average nucleotide identity (ANI) pair-comparison matrix for *Pseudomonas* sp. strain FIT28^T and its most closely related species. Values are expressed as percentages of identity.

Table 2: Digital DNA-DNA hybridization (dDDH) values between the genomes of *Pseudomonas* sp. strain FIT28^T and its most closely related species.

Table 3: Differential biochemical phenotypes between *Pseudomonas* sp. strain FIT28^T and its closest relative species. Species 1, strain FIT28^T; 2, *P. zeae* OE48.2^T [46]*;* 3, *P. tensinigenes* ZA5.3^T [46]; 4, *P. crudilactis* UCMA 17988^T [45], 5, *P. helmanticensis* OHA11^T (= CECT 8548); 6, *P. baetica* a390^T (= CECT 7720); 7, *P. iridis* P42^T [47]; 8, *P. atagonensis* PS14^T (= CECT 9940); 9, *P. koreensis* DSM 16610^T [37–41, 44]; 10, *P. granadensis* LMG 27940^T [37, 39, 42, 43]; 11*, P. hamedanensis* SWRI65^T [46]; 12, *P. atacamensis* LMG 34516^T [37] and 13, *P. moraviensis* DSM 16007^T [37, 39, 40, 42, 44]. Results are summarized as positive (+), negative (-), weak or uncertain (/), and not described previously (ND). API Zym enzymatic activities were scored as strong (+++), middle (++), weak (+), and uncertain (/).

Table 4: Percentages of cellular fatty acids composition of strain FIT28^T and its relative's species. Specie 1, strain FIT28^T; 2, *P. crudilactis* UCMA 17988^T [45]; 3, *P. helmanticensis* OHA11^T [50]; 4, *P. baetica* a390^T [40]; 5, *P. atagonensis* PS14^T [49]; 6, *P. koreensis* DSM 16610^T [39, 41, 43]; 7, *P. granadensis* LMG 27940^T [39, 43]; 8, *P. iridis* P42^T [47]; 9, *P. atacamensis* LMG 34516^T [37] and 10, *P. moraviensis* DSM 16007^T [39, 44]. Not detected fatty acids are indicated in (-) and traces with (TR).

Figure 1

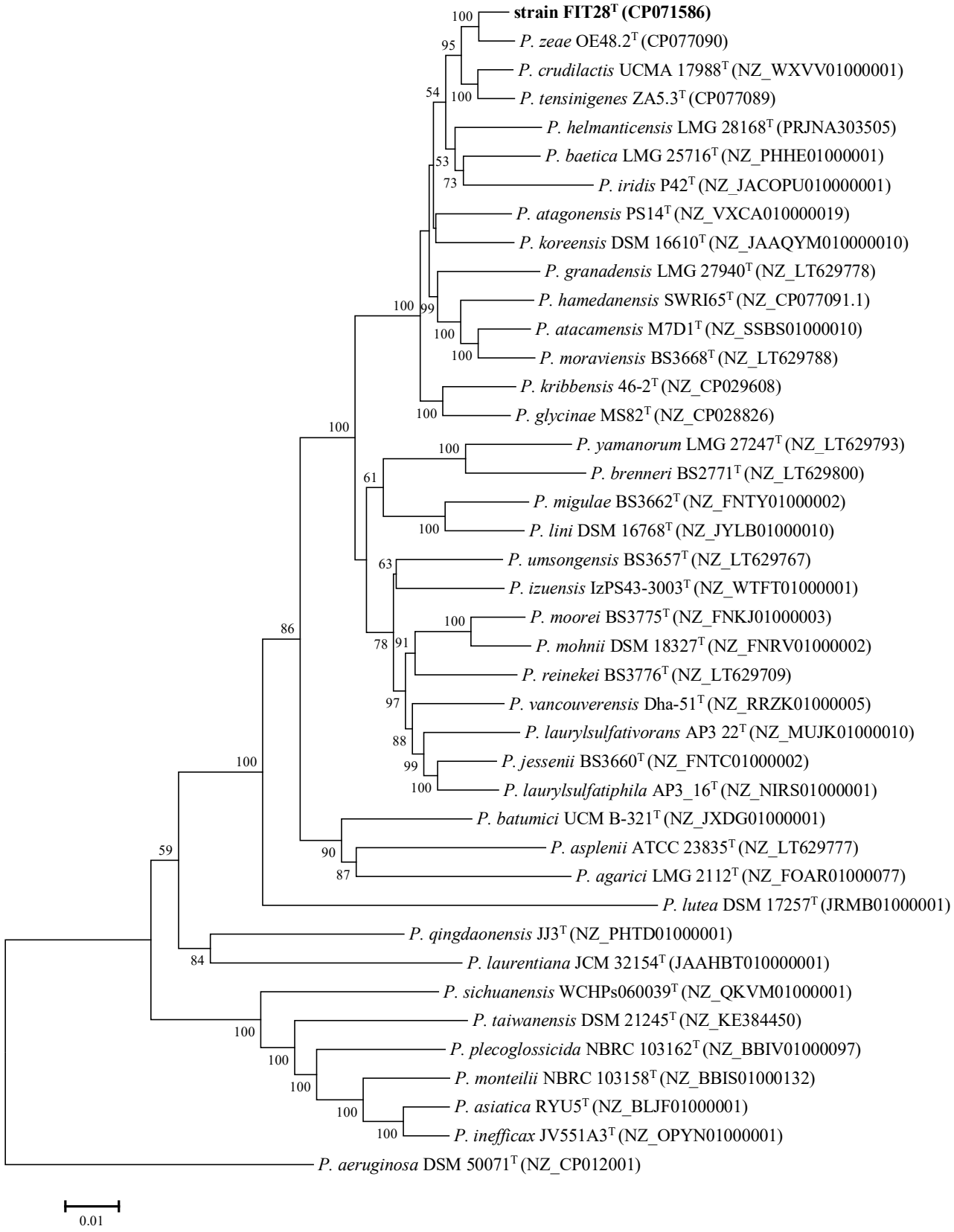
strain FIT28T (CP071586)
P. zeae OE48.2T (CP077090)
P. crudilactis UCMA 17988T (NZ_WXVV01000001)
P. tensinigenes ZA5.3T (CP077089)
P. helmanticensis LMG 28168T (PRJNA303505)
P. baetica LMG 25716T (NZ_PHHE01000001)
P. iridis P42T (NZ_JACOPU010000001)
P. atagonensis PS14T (NZ_VXCA010000019)
P. koreensis DSM 16610T (NZ_JAAQYM010000010)
P. granadensis LMG 27940T (NZ_LT629778)
P. hamedanensis SWRI65T (NZ_CP077091.1)
P. atacamensis M7D1T (NZ_SSBS01000010)
P. moraviensis BS3668T (NZ_LT629788)
P. kribbensis 46-2T (NZ_CP029608)
P. glycinae MS82T (NZ_CP028826)
P. yamanorum LMG 27247T (NZ_LT629793)
P. brenneri BS2771T (NZ_LT629800)
P. migulae BS3662T (NZ_FNTY01000002)
P. lini DSM 16768T (NZ_JYLB01000010)
P. umsongensis BS3657T (NZ_LT629767)
P. izuensis IzPS43-3003T (NZ_WTFT01000001)
P. moorei BS3775T (NZ_FNKJ01000003)
P. mohnii DSM 18327T (NZ_FNRV01000002)
P. reinekei BS3776T (NZ_LT629709)
P. vancouverensis Dha-51T (NZ_RRZK01000005)
P. laurylsulfativorans AP3 22T (NZ_MUJK01000010)
P. jessenii BS3660T (NZ_FNTC01000002)
P. laurylsulfatiphila AP3_16T (NZ_NIRS01000001)
P. batumici UCM B-321T (NZ_JXDG01000001)
P. asplenii ATCC 23835T (NZ_LT629777)
P. agarici LMG 2112T (NZ_FOAR01000077)
P. lutea DSM 17257T (JRMB01000001)
P. qingdaonensis JJ3T (NZ_PHTD01000001)
P. laurentiana JCM 32154T (JAAHBT010000001)
P. sichuanensis WCHPs060039T (NZ_QKVM01000001)
P. taiwanensis DSM 21245T (NZ_KE384450)
P. plecoglossicida NBRC 103162T (NZ_BBIV01000097)
P. monteilii NBRC 103158T (NZ_BBIS01000132)
P. asiatica RYU5T (NZ_BLJF01000001)
P. inefficax JV551A3T (NZ_OPYN01000001)
P. aeruginosa DSM 50071T (NZ_CP012001)
0.01

Figure 2

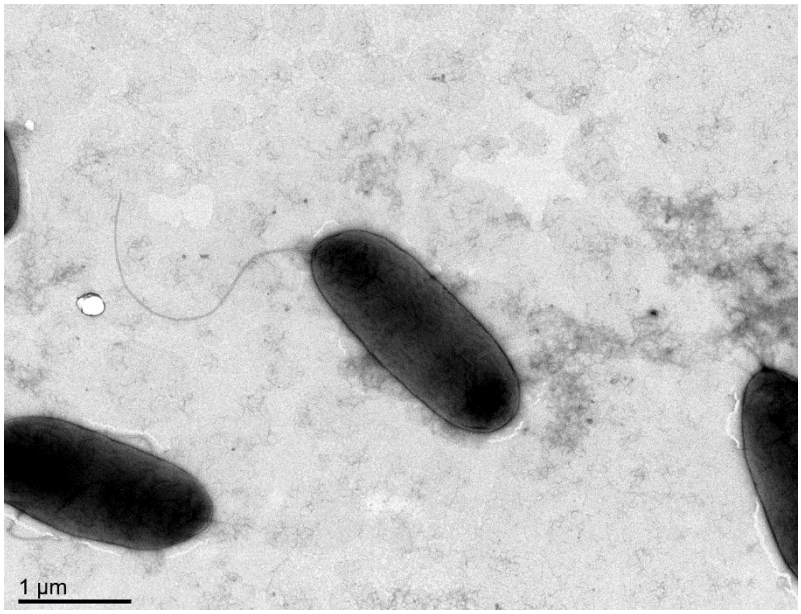

Figure 3

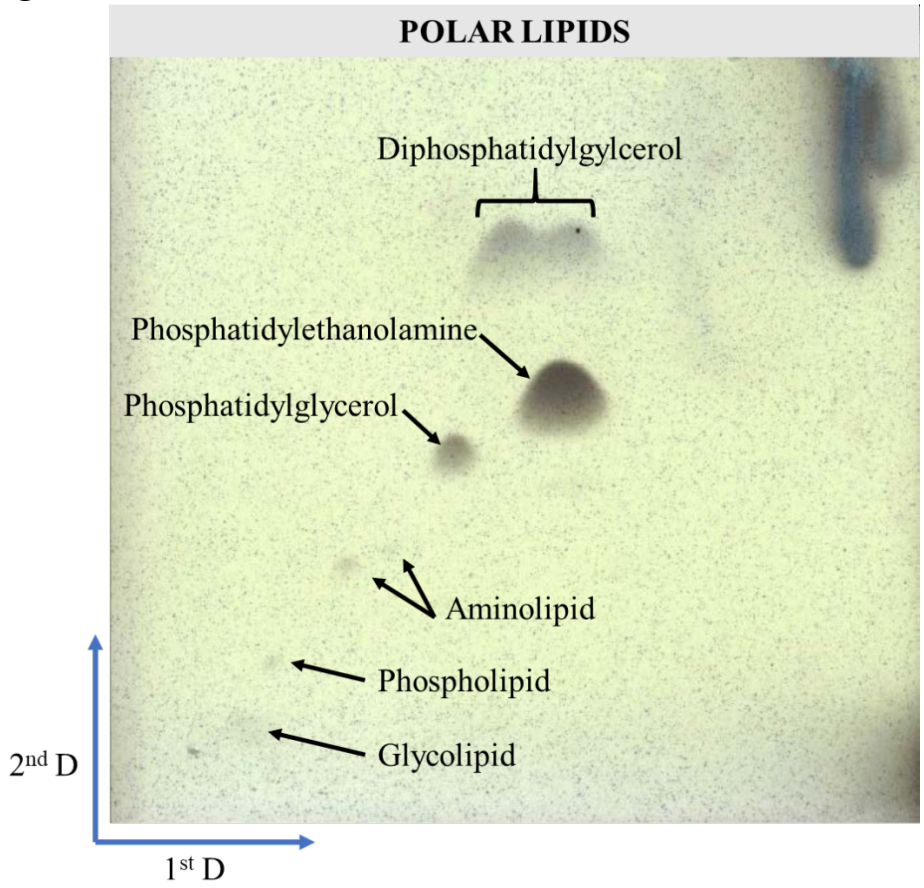
POLAR LIPIDS
Diphosphatidylgylcerol
Phosphatidylethanolamine
Phosphatidylglycerol
Aminolipid
Phospholipid
Glycolipid
2nd D
1st D

Table 1

ANI

	FIT28^{T}	48.2^{T}	ZA 5.3^{T}	UCMA 17988^{T}	OHA11^{T}	a390^{T}	PS14^{T}	DSM 16610^{T}	P42^{T}	LMG 27940^{T}	M7D^{T}	BS3668^{T}	SWRI65^{T}
Pseudomonas sp. FIT28^{T}	100	95.23	91.50	91.13	88.96	88.12	87.73	87.62	87.38	87.21	86.83	86.83	86.64
P. zeae OE48.2^{T}	95.23	100	91.38	91.27	89.05	88.19	88.06	87.73	87.43	87.36	86.97	86.90	86.77
P. tensinigenes ZA5.3^{T}	91.50	91.38	100	93.48	89.05	88.24	88.11	87.63	87.65	87.41	86.99	86.72	86.83
P. crudilactis UCMA 17988^{T}	91.13	91.27	93.48	100	89.07	88.07	87.98	87.54	87.59	87.21	86.82	86.64	86.68
P. helmanticensis OHA11^{T}	88.96	89.05	89.05	89.07	100	87.86	87.82	87.41	87.41	86.93	86.86	86.63	86.79
P. baetica a390^{T}	88.12	88.19	88.24	88.07	87.86	100	87.81	87.73	88.35	86.71	86.56	86.36	86.87
P. atagonensis PS14^{T}	87.73	88.06	88.11	87.98	87.82	87.81	100	87.60	87.47	86.64	86.62	86.42	86.51
P. koreensis DSM 16610^{T}	87.62	87.73	87.63	87.54	87.41	87.73	87.60	100	87.16	86.69	86.55	86.49	86.44
P. iridis P42^{T}	87.38	87.43	87.65	87.59	87.41	88.35	87.47	87.16	100	86.19	86.22	86.05	86.02
P. granadensis LMG 27940^{T}	87.21	87.36	87.41	87.21	86.93	86.71	86.64	86.69	86.19	100.00	87.20	87.06	86.94
P. atacamensis M7D^{T}	86.83	86.97	86.99	86.82	86.86	86.56	86.62	86.55	86.22	87.20	100	91.79	88.04
P. moraviensis BS3668^{T}	86.83	86.90	86.72	86.64	86.63	86.36	86.42	86.49	86.05	87.06	91.79	100	88.15
P. hamedanensis SWRI65^{T}	86.64	86.77	86.83	86.68	86.79	86.87	86.51	86.44	86.02	86.94	88.04	88.15	100

Table 2

Species	Strain	dDDH to strain FIT28^T
P. zeae	OE48.2^T	63.4% [60.5 – 66.2%]
P. tensinigenes	ZA5.3^T	46.7% [44.2 – 49.3%]
P. crudilactis	UCMA 17988^T	45.4% [42.8 – 48.0%]
P. helmanticensis	OHA11^T	38.6% [36.1 – 41.1%]
P. baetica	a390^T	36.4% [34.0 – 38.9%]
P. koreensis	DSM 16610^T	35.1% [32.6 – 37.6%]
P. atagonensis	PS14^T	35.0% [32.5 – 37.5%]
P. iridis	P42^T	34.7% [32.3 – 37.2%]
P. granadensis	LMG 27940^T	34.2% [31.7 – 36.7%]
P. atacamensis	M7D^T	33.8% [31.3 – 36.3%]
P. hamedanensis	SWRI65^T	33.5% [31.1 – 36.0%]
P. moraviensis	BS3668^T	33.3% [30.9 – 35.8%]

Table 3

Characteristics	**1**	**2**	**3**	**4**	**5**	**6**	**7**	**8**	**9**	**10**	**11**	**12**	**13**
Fluorescence on King's B media	+	ND	ND	-	+	+	+	+	+	+	ND	+	+
Growth at 37 ◦C	-	ND	ND	-	-	-	+	-	+	+	ND	+	+
Growth on 4% NaCl	+	/	-	+	+	+	+	+	+	+	+	ND	+
Growth on 6% NaCl	+	ND	ND	-	-	-	+	-	+	-	ND	-	+
Oxidation of:													
Glucose	+	+	+	+	+	+	+	+	+	+	+	+	-
Melibiose	+	/	+	+	+	+	-	-	-	+	/	ND	-
D-Arabitol	+	-	/	+	+	+	+	+	+	+	/	ND	+
D-Fructose	+	/	-	+	+	+	+	+	+	+	+	ND	+
D-Galactose	+	+	+	+	+	+	ND	+	+	+	+	-	+
D-Galacturonic acid	/	/	/	+	/	/	+	/	-	-	/	ND	-
D-Gluconic acid	+	/	/	+	+	+	+	+	+	ND	+	ND	+
D-Glucuronic acid	/	/	+	-	+	/	+	/	+	-	/	ND	-
D-Lactic acid methyl ester	/	-	-	+	/	+	-	/	+	ND	-	ND	+
D-Mannitol	+	-	/	+	+	+	+	+	+	+	/	ND	+
D-Mannose	+	+	+	+	+	+	+	+	+	+	+	ND	+
D-Saccharic acid	+	/	+	+	+	+	+	+	+	+	+	ND	+
D-Trehalose	-	-	-	-	-	+	+	-	-	+	-	+	+
Formic acid	+	-	-	+	+	+	-	+	+	-	/	ND	-
Glucuronamide	+	+	+	+	+	+	+	+	+	+	+	ND	+
Inosine	+	/	/	+	+	+	+	+	+	+	+	ND	+

L-Alanine	+	/	+	+	+	+	+	+	+	ND	+	ND	+
L-Galactonic acid lactone	/	+	+	+	/	+	+	/	+	+	/	ND	+
L-Pyroglutamic acid	+	-	+	+	+	+	+	+	+	+	+	ND	+
Pectin	+	-	-	+	/	/	-	/	ND	ND	-	ND	+
p-Hydroxyphenylacetic acid	-	-	-	-	-	-	-	-	-	-	-	ND	-
Propionic acid	+	-	/	-	+	+	+	+	+	+	/	ND	+
Sucrose	+	-	-	-	-	-	-	/	+	+	-	ND	ND
α-Ketobutyric acid	/	-	-	-	+	/	-	/	+	/	/	ND	+
α-Ketoglutaric acid	+	+	+	-	+	+	+	+	+	+	+	ND	+
γ-Hydroxybutyric acid	+	-	-	+	/	/	-	/	-	ND	-	ND	-
Acetic acid	+	+	+	-	+	+	+	+	+	/	+	ND	+
Enzymatic activities													
Catalase	+	+	+	+	+	+	+	+	+	+	+	+	+
Cytochrome oxidase	+	+	+	+	+	+	+	+	+	+	+	+	+
Gelatin hydrolisis	+	-	-	-	-	+	+	+	+	+	-	-	+

Table 4

Fatty acid	1	2	3	4	5	6	7	8	9	10
$C_{10:0}$ 3-OH	3.09	4.0	2.4	3.44	3.2	4.2	3.2	4.16	TR	2.6
$C^{12:0}$ 2-OH	3.3	5.2	4.9	5.54	5.3	6.2	4.7	5.36	10.27	4.9
$C_{12:0}$ 3-OH	3.61	4.2	2.9	3.23	4.5	5.1	2.5	4.28	TR	4.1
$C_{12:0}$	3.26	1.4	2	1.68	1.6	5	1.5	1.7	TR	2.1
$C_{16:0}$	29.56	33.7	31.9	29.43	32.8	20	31.9	35.97	24.98	28.8
$C_{17:0}$ cyclo	3.06	2.8	5.1	3.15	11.5	1.5	6.9	7.48	TR	2.4
$C_{18:1}$ ω7c	17.15	-	15.6	8.5	ND	13.4	12.4	-	9.53	17.3
$C_{18:0}$	1.55	-	0.8	0.34	TR	1.7	-	TR	ND	0.5
Summed feature 3 ($C_{16:1}$ ω7c/$C_{15:0}$ iso 2-OH)	33.9	36.2	32.9	42.4	27.2	41.9	35.6	29.86	28.67	34.2

REFERENCES

1. **Peix A, Ramírez-Bahena MH, Velázquez E**. The current status on the taxonomy of *Pseudomonas* revisited: An update. Infect Genet Evol. 2018;57:106-116. https://doi.org/10.1016/j.meegid.2017.10.026.
2. **Chun J, Oren A, Ventosa A, Christensen H, Arahal DR, *et al.*** Proposed minimal standards for the use of genome data for the taxonomy of prokaryotes. Int J Syst Evol Microbiol. 2018;68(1):461-466. https://doi.org/10.1099/ijsem.0.002516.
3. **Gomila M, Peña A, Mulet M, Lalucat J, García-Valdés E**. Phylogenomics and systematics in *Pseudomonas*. Front Microbiol. 2015;6:214. https://doi.org/10.3389/fmicb.2015.00214.
4. **Garrido-Sanz D, Meier-Kolthoff JP, Göker M, Martín M, Rivilla R, *et al.*** Genomic and Genetic Diversity within the *Pseudomonas fluorescens* Complex. PLoS One. 2016;11(2):e0150183. https://doi.org/10.1371/journal.pone.0150183.
5. **Hesse C, Schulz F, Bull CT, Shaffer BT, Yan Q, *et al.*** Genome-based evolutionary history of *Pseudomonas* spp. Environ Microbiol. 2018;20(6):2142-2159. https://doi.org/10.1111/1462-2920.14130.
6. **Franco-Duarte R, Černáková L, Kadam S, Kaushik KS, Salehi B, *et al.*** Advances in chemical and biological methods to identify microorganisms-from past to present. Microorganisms. 2019;7(5):130. https://doi.org/10.3390/microorganisms7050130.
7. **Scales BS, Dickson RP, Lipuma JJ, Huffnagle GB.** Microbiology, genomics, and clinical significance of the *Pseudomonas fluorescens* species complex, an unappreciated colonizer of humans. Clin Microbiol Rev. 2014;27(4):927-48. https://doi.org/10.1128/CMR.00044-14
8. **Gera Hol WH, Martijn Bezemer T, Biere A**. Getting the ecology into interactions between plants and the plant growth-promoting bacterium *Pseudomonas fluorescens*. Front Plant Sci. 2013;4:81. https://doi.org/10.3389/fpls.2013.00081.
9. **Singh M, Kumar A, Singh R, Pandey KD.** Endophytic bacteria: a new source of bioactive compounds. 3 Biotech. 2017;7(5):315. https://doi.org/10.1007/s13205-017-0942-z.
10. **Doyle JJ, Doyle JL**. A rapid DNA isolation procedure for small quantities of fresh leaf tissue. Phytochem. Bull. 1987;19(1):11–15.
11. **Minas K, Mcewan NR, Newbold CJ, Scott KP**. Optimization of a high-throughput CTAB-based protocol for the extraction of qPCR-grade DNA from rumen fluid, plant and bacterial pure cultures. FEMS Microbiol Lett. 2011;325(2):162-9. https://doi.org/10.1111/j.1574-6968.2011.02424.x.
12. **Bodenhausen N, Horton MW, Bergelson J**. Bacterial communities associated with the leaves and the roots of *Arabidopsis thaliana*. PLoS One. 2013;8(2):e56329. https://doi.org/10.1371/journal.pone.0056329.
13. **Cole JR, Wang Q, Fish JA, Chai B, McGarrell DM, *et al.*** Ribosomal Database Project: data and tools for high throughput rRNA analysis. Nucleic Acids Res. 2014;42(Database issue):D633-42. https://doi.org/10.1093/nar/gkt1244.
14. **Wick RR, Judd LM, Gorrie CL, Holt KE**. Unicycler: Resolving bacterial genome assemblies from short and long sequencing reads. PLoS Comput Biol. 2017;13(6):e1005595. https://doi.org/10.1371/journal.pcbi.1005595.
15. **Hyatt D, Chen GL, LoCascio PF, Land ML, Larimer FW, *et al***. Prodigal: prokaryotic gene recognition and translation initiation site identification. BMC Bioinformatics. 2010;11:119. https://doi.org/10.1186/1471-2105-11-119.
16. **Lee I, Chalita M, Ha SM, Na SI, Yoon SH, *et al.*** ContEst16S: an algorithm that identifies contaminated prokaryotic genomes using 16S RNA gene sequences. Int J Syst Evol Microbiol. 2017;67(6):2053-2057. https://doi.org/10.1099/ijsem.0.001872.
17. **Yoon SH, Ha SM, Kwon S, Lim J, Kim Y, *et al.*** Introducing EzBioCloud: a

taxonomically united database of 16S rRNA gene sequences and whole-genome assemblies. Int J Syst Evol Microbiol. 2017;67(5):1613-1617. https://doi.org/10.1099/ijsem.0.001755.
18. **Glaeser SP, Kämpfer P**. Multilocus sequence analysis (MLSA) in prokaryotic taxonomy. Syst Appl Microbiol. 2015;38(4):237-45. https://doi.org/10.1016/j.syapm.2015.03.007.
19. **Edgar RC**. MUSCLE: multiple sequence alignment with high accuracy and high throughput. Nucleic Acids Res. 2004;32(5):1792-7. https://doi.org/10.1093/nar/gkh340.
20. **Nordberg H, Cantor M, Dusheyko S, Hua S, Poliakov A, *et al.*** .The genome portal of the Department of Energy Joint Genome Institute: 2014 updates. Nucleic Acids Res. 2014;42(Database issue):D26-31. https://doi.org/10.1093/nar/gkt1069.
21. **Wattam AR, Abraham D, Dalay O, Disz TL, Driscoll T, *et al.*** PATRIC, the bacterial bioinformatics database and analysis resource. Nucleic Acids Res. 2014;42(Database issue):D581-91. https://doi.org/10.1093/nar/gkt1099.
22. **Kumar S, Stecher G, Li M, Knyaz C, Tamura K**. MEGA X: Molecular Evolutionary Genetics Analysis across Computing Platforms. Mol Biol Evol. 2018;35(6):1547-1549. https://doi.org/10.1093/molbev/msy096.
23. **Felsenstein J**. Confidence limits on phylogenesis: An approach using the bootstrap. Evolution. 1985;39(4):783-791. https://doi.org/10.1111/j.1558-5646.1985.tb00420.x.
24. **Mulet M, Gomila M, Lemaitre B, Lalucat J, García-Valdés E.** Taxonomic characterisation of *Pseudomonas* strain L48 and formal proposal of *Pseudomonas entomophila* sp. nov. Syst Appl Microbiol. 2012; 35(3):145–149. https://doi.org/10.1016/j.syapm.2011.12.003.
25. **Na SI, Kim YO, Yoon SH, Ha S min, Baek I, *et al.*** UBCG: Up-to-date bacterial core gene set and pipeline for phylogenomic tree reconstruction. J Microbiol. 2018; 56(4):280-285. https://doi.org/10.1007/s12275-018-8014-6
26. **Mulet M, Lalucat J, García-Valdés E.** DNA sequence-based analysis of the *Pseudomonas* species. Environ Microbiol. 2010;12(6):1513-1530. https://doi.org/10.1111/j.1462-2920.2010.02181.x.
27. **Scales BS, Erb-Downward JR, Huffnagle IM, LiPuma JJ, Huffnagle GB**. Comparative genomics of *Pseudomonas fluorescens* subclade III strains from human lungs. BMC Genomics. 2015;16:1032. https://doi.10.1186/s12864-015-2261-2.
28. **Suzuki S, Kakuta M, Ishida T, Akiyama Y**. GHOSTX: an improved sequence homology search algorithm using a query suffix array and a database suffix array. PLoS One. 2014;9(8):e103833. https://doi.org/10.1371/journal.pone.0103833.
29. **Laslett D, Canback B**. ARAGORN, a program to detect tRNA genes and tmRNA genes in nucleotide sequences. Nucleic Acids Res. 2004;32(1):11-6. https://doi.org/10.1093/nar/gkh152.
30. **Lee I, Kim YO, Park SC, Chun J**. OrthoANI: An improved algorithm and software for calculating average nucleotide identity. Int J Syst Evol Microbiol. 2016;66(2):1100-1103. https://doi.org/10.1099/ijsem.0.000760.
31. **Richter M, Rosselló-Móra R, Oliver Glöckner F, Peplies J**. JSpeciesWS: a web server for prokaryotic species circumscription based on pairwise genome comparison. Bioinformatics. 2016; 32(6):929–931. https://doi.org/10.1093/bioinformatics/btv681.
32. **Ciufo S, Kannan S, Sharma S, Badretdin A, Clark K, et al.** Using average nucleotide identity to improve taxonomic assignments in prokaryotic genomes at the NCBI. Int J Syst Evol Microbiol. 2018; 68(7):2386-2392. https://doi.org/10.1099/ijsem.0.002809.
33. **Meier-Kolthoff JP, Auch AF, Klenk HP, Göker M**. Genome sequence-based species delimitation with confidence intervals and improved distance functions. BMC Bioinformatics. 2013;14:60. https://doi.org/10.1186/1471-2105-14-60.
34. **Auch AF, Klenk H-P, Göker M.** Standard operating procedure for calculating

445 genome-to-genome distances based on high-scoring segment pairs. Stand Genomic Sci.
446 2010;2(1):142-8. https://doi.org/10.4056/sigs.541628.
447 35. **Donnarumma G, Buommino E, Fusco A, Paoletti I, Auricchio L, *et al.*** Effect of
448 temperature on the shift of *Pseudomonas fluorescens* from an environmental microorganism to
449 a potential human pathogen. Int J Immunopathol Pharmacol. 2010;23(1):227-34.
450 https://doi.org/10.1177/039463201002300120.
451 36. **King E, Ward MK, Raney DE**. Two simple media for the demonstration of pyocyanin
452 and fluorescin. J Lab Clin Med. 1954;44(2):301–7.
453 37. **Poblete-Morales M, Carvajal D, Almasia R, Michea S, Cantillana C, *et al.*** *Pseudomonas atacamensis* sp. nov., isolated from the rhizosphere of desert bloom plant in the
455 region of Atacama, Chile. Antonie Van Leeuwenhoek. 2020;113(8):1201-1211.
456 https://doi.org/10.1007/s10482-020-01427-0.
457 38. **Kwon SW, Kim JS, Park IC, Yoon SH, Park DH, *et al.*** *Pseudomonas koreensis* sp.
458 nov., *Pseudomonas umsongensis* sp. nov., and *Pseudomonas jinjuensis* sp. nov., novel species
459 from farm soils in Korea. Int J Syst Evol Microbiol. 2003;53(1):21-27.
460 https://doi.org/10.1099/ijs.0.02326-0.
461 39. **Pascual J, García-Lopez M, Bills GF, Genilloud O.** *Pseudomonas granadensis* sp.
462 nov., a new bacterial species isolated from the Tejeda, Almijara and Alhama Natural Park,
463 Granada, Spain. Int J Syst Evol Microbiol. 2015;65(2):625-632.
464 https://doi.org/10.1099/ijs.0.069260-0.
465 40. **López JR, Diéguez AL, Doce A, de la Roca E, de la Herran R, *et al.*** *Pseudomonas
466 baetica* sp. nov., a fish pathogen isolated from wedge sole, *Dicologlossa cuneata* (Moreau). Int
467 J Syst Evol Microbiol. 2012;62(4):874-882. https://doi.org/10.1099/ijs.0.030601-0.
468 41. **Cámara B, Strömpl C, Verbarg S, Spröer C, Pieper DH, *et al.*** *Pseudomonas
469 reinekei* sp. nov., *Pseudomonas moorei* sp. nov., and *Pseudomonas mohnii* sp. nov., novel
470 species capable of degrading chlorosalicylates or isopimaric acid. Int J Syst Evol Microbiol.
471 2007;57(5):923-931. https://doi.org/10.1099/ijs.0.64703-0.
472 42. **Jia J, Wang X, Deng P, Ma L, Baird SM, *et al.*** *Pseudomonas glycinae* sp. nov.,
473 isolated from the soybean rhizosphere. MicrobiologyOpen. 2020;9(9):e1101.
474 https://doi.org/10.1002/mbo3.1101.
475 43. **Chang DH, Rhee MS, Kim JS, Lee Y, Park MY, *et al.*** *Pseudomonas kribbensis* sp.
476 nov., isolated from garden soils in Daejeon, Korea. Antonie Van Leeuwenhoek.
477 2016;109(11):1433-1446. https://doi.org/10.1007/s10482-016-0743-0.
478 44. **Tvrzová L, Schumann P, Spröer C, Sedláček I, Páčová Z, *et al.*** *Pseudomonas
479 moraviensis* sp. nov., and *Pseudomonas vranovensis* sp. nov., soil bacteria isolated on
480 nitroaromatic compounds, and emended description of *Pseudomonas asplenii*. Int J Syst Evol
481 Microbiol. 2006;56(11):2657-2663. https://doi.org/10.1099/ijs.0.63988-0
482 45. **Schlusselhuber M, Girard L, Cousin FJ, Lood C, de Mot R, *et al.*** *Pseudomonas
483 crudilactis* sp. nov., isolated from raw milk in France. Antonie Van Leeuwenhoek.
484 2021;114(6):719-730. https://doi.org/10.1007/s10482-021-01552-4.
485 46. **Girard L, Lood C, Höfte M, Vandamme P, Rokni-Zadeh H, *et al.*** The ever-
486 expanding *Pseudomonas* genus: Description of 43 new species and partition of the
487 *Pseudomonas putida* group. Microorganisms. 2021;9(8):1766.
488 https://doi.org/10.3390/microorganisms9081766.
489 47. **Duman M, Mulet M, Altun S, Burcin Saticioglu I, Gomila M, *et al***. *Pseudomonas
490 anatoliensis* sp. nov and *Pseudomonas iridis* sp. nov. isolated from fish. Syst Appl Microbiol.
491 2021;44(3):126198. https://doi.org/10.1016/j.syapm.2021.126198.
492 48. **Acosta-Martínez V, Tabatabai MA**. Arylamidase activity in soils: Effect of trace
493 elements and relationships to soil properties and activities of amidohydrolases. Soil Biol
494 Biochem. 2001;33(1):17–23. https://doi.org/10.1016/S0038-0717(00)00109-7.

49. **Morimoto Y, Uwabe K, Tohya M, Hiramatsu K, Kirikae T, *et al.*** *Pseudomonas atagonensiss* sp. nov., and *Pseudomonas akappagea* sp. nov., New Soil Bacteria Isolated from Samples on the Volcanic Island Izu Oshima, Tokyo. Curr Microbiol. 2020;77(8):1909-1915. https://doi.org/10.1007/s00284-020-01943-2.
50. **Ramírez-Bahena MH, Cuesta MJ, Flores-Félix JD, Mulas R, Rivas R, *et al.*** *Pseudomonas helmanticensis* sp. nov., isolated from forest soil. Int J Syst Evol Microbiol. 2014;64(Pt 7):2338-2345. https://doi.org/10.1099/ijs.0.063560-0